Applied Physics A (2022) 128:191
https://doi.org/10.1007/s00339-022-05315-4

Applied Physics A
Materials Science & Processing

Effect of microstructure on thermal field distribution of absorption glass with nanosecond laser-irradiated

Tianlu Wei[1] · Bo Dong[2,3] · Shuo Hu[2] · Haozhe Liu[3] · Jiaxuan Chen[2] · Yilan Jiang[4] · Xiaogang Chang[2] · Yunlong Du[2]

Received: 13 July 2021 / Accepted: 18 January 2022

Abstract
Stray light absorption glass to improve high-energy laser systems' service life becomes a meaningful method. The relationship between microstructure of the surface of absorption glass and laser-induced damage is crucial and still not fully understood. This paper investigates the effect of depth and width of V-shaped microstructure surface on the thermal field of absorption glass by establishing an electromagnetic heat coupling model. The graphs that represent individual conditions versus extreme temperature are achieved. The thermal distribution of the depth-to-width ratio in this microstructure which could avoid the higher temperature is mapped.

Keywords Microstructure · Depth-width ratio · Thermal field · Nanosecond pulse laser

1 Introduction

In high-energy laser systems, stray light scattering is an urgent need like in inertial confinement fusion (ICF) [1–4] field that bothers many scholars. Because the surface of optical parts is not idealized, there are various defects on surfaces and subsurfaces [5, 6]. When laser irradiates optical components, a few beam pieces will always be scattered. The system amplifies the stray light, which may ablate the surface of the structural material, then generate pollutants that fill the space. It causes significant damage to the optical parts and shortens their working life when pollution adheres to optical elements' surface. The US National Ignition Facility (NIF) [7, 8] uses more than 7360 large-caliber optical components, including precision optical components. The total area of these components is up to 4000 square meters [9]. In the NIF device, the research results show that the contaminants reduced the optical element's laser damage threshold by about 60 percent [10]. The contaminations are derived from the microstructure of the optical device and the interaction with stray light. Therefore, it is necessary to study the absorption of stray light on designed shape of the device.

Since 1964, Giuliano et al. studied the mechanism of lasers and materials. Laser damage materials have been an important research direction [11]. In 1973, Bloembergen et al. studied the effects of cracks, pores, and foreign particles on the ability to damage lasers [12]. In 1975, Lawn et al. classified the microcracks on the surface of optical elements, analyzed the stress distribution in the area near the microcracks, and laid the foundation for subsequent theoretical simulations [13]. Genin et al. found that the light field enhancement effect is related to the incident wave's polarization direction, incident angle, and crack geometry [14]. Rubenchik et al. pointed out that surface point defects and surface microcracks are the leading causes of laser damage, revealing microcracks and damage growth relationship [15]. According to Feit's research, surface damage is divided into three main sections. These include thermal damage caused by absorbing surface impurities, field damage caused by defective optical field

Tianlu Wei and Bo Dong contribute equally to the article.

✉ Jiaxuan Chen
lrimohs9838631@163.com

✉ Yilan Jiang
jiangyilan1023@163.com

[1] School of Mechanical and Vehicle Engineering, Bengbu University, 1866 Caoshan Street, Bengbu 233000, China

[2] School of Mechatronics Engineering, Harbin Institute of Technology, Harbin 150001, China

[3] Center for High Pressure Science and Technology Advanced Research, Haidian, Beijing 100094, China

[4] Laser Fusion Research Center, China Academy of Engineering Physics, Mianyang 621900, China

Published online: 11 February 2022

modulation, and surface defects that weaken the mechanical properties of the optical element and lower the damage threshold [16]. At the same time, a reasonable surface microstructure has a significant effect on the absorption of stray light. Some materials can be highly absorptive ones by the formation of surface micro/nanostructures, called "black metal" [17], e.g., black gold, platinum, titanium, tungsten, and aluminum [18–21]. In addition, black glass is used as the main material to absorb stray light [22].

Under the current processing conditions, a practical approach for absorbing stray light on the material's surface—building a microstructure array—can be used to limit the damage caused by stray light on the material's surface. The energy of the primary stray light is not very high, and it can be weakened many times through the absorption layer by layer. However, the problem is that the microstructure will reduce the damage threshold of the material. Therefore, it is necessary to find a balance between the reduction of the material damage threshold and the efficiency of the microstructure to absorb stray light. A simulation of the thermal field of laser-irradiated materials by micro-nano structures is performed to explore the change rule of the thermal distribution of absorption glass and guide the construction and optimization of subsequent microstructures.

Table 1 Laser parameters

Spot area mm^2	Optical splitting ratio	Laser wavelength nm	Laser pulse width ns	Energy density J/cm^2
0.80	22.50	355.00	6.00	6

2 Model and simulation

Using the solid heat transfer and solid mechanics modules in the multi-physics coupling software, the model of temperature and electric field during laser irradiation of materials is achieved, by solving partial differential equations based on the finite element theory.

The laser ablation models were carried out using a SAGA (Nd: YAG) laser, with a wavelength of 355 nm and a spot area of 0.8 mm^2. The relevant parameters are shown in Table 1.

A Gauss nanosecond pulse laser is adopted, and the laser pulse width is 6 ns. Figure 1 shows a spatial distribution of the Gauss nanosecond pulse laser.

The HWB3 of absorption series glass is selected for the application in high-energy laser systems due to the excellent absorption performance for the 351 nm wavelength laser. The laser action time is on the nanosecond level, and the thermal conductivity of air is relatively minor. Therefore, it is assumed that the thermophysical parameters of the material do not change with temperature and the convective heat dissipation between the material. The role of air before laser-irradiated surfaces is ignored. The thermophysical parameters of the materials are exhibited in Table 2.

The laser spot radius in the model is 500 μm. The workpiece radius is set to 1400 μm and the thickness to 200 μm. The laser loading method is a single pulse, and the loading time is a pulse width of 6 ns. After a pulse width of 6 ns, the laser stops loading, and laser is 100 ns delayed. The meshing of the model adopts a free triangle mesh, and appropriate mesh encryption is performed in the radial and axial directions. The solver time step is set as 0.2 ns to ensure

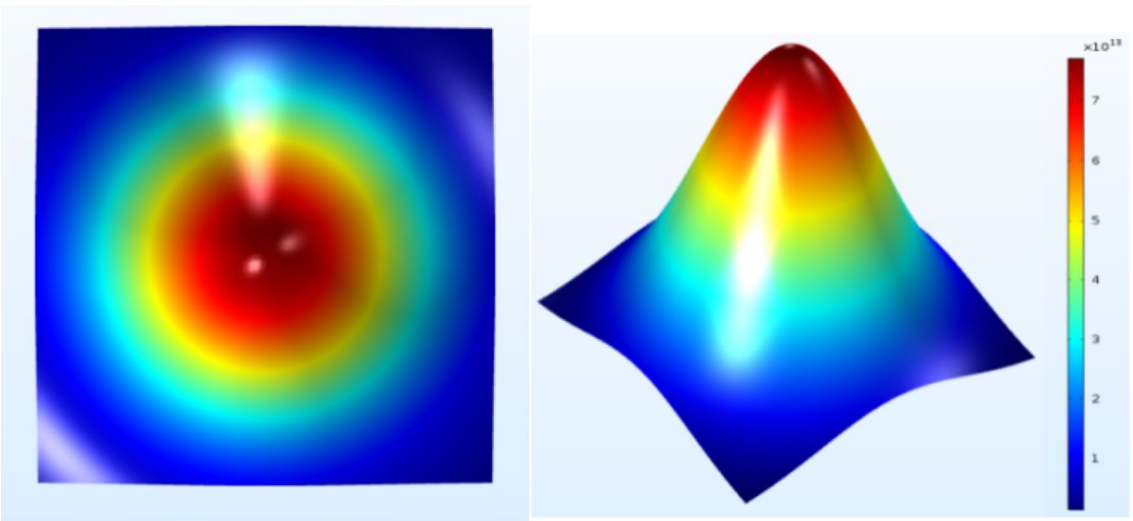

Fig. 1 Gaussian beam spatial distribution

the precision of calculated result. A brief description of the model is shown in Fig. 2. The V-shaped groove was scratched as the main research object on the ideal surface. The width is denoted as *w*, and the depth is denoted as *d*.

A nanosecond laser with energy density of 6 J/cm^2 is loaded on the model's surface. The three-dimensional thermal field is shown in Fig. 3. It can be seen from the illustration that the temperature shows a ring-shaped temperature band, and the whole is in an axis-symmetric state, which is the same as the spatial distribution state of the laser. Radial light intensity follows a Gaussian

Table 2 Thermophysical parameters.

Density g/cm3	Specific heat capacity J/(kg K)	Thermal conductivity coefficient W/(m K)	Coefficient of expansion 10^{-6} K^{-1}	Absorption coefficient m^{-1}
2.50	840	0.76	6.5	3176
Young's modulus GPa	Poisson's ratio	Compression limit MPa	Tensile limit MPa	Melting point K
55	0.25	800	45	1750

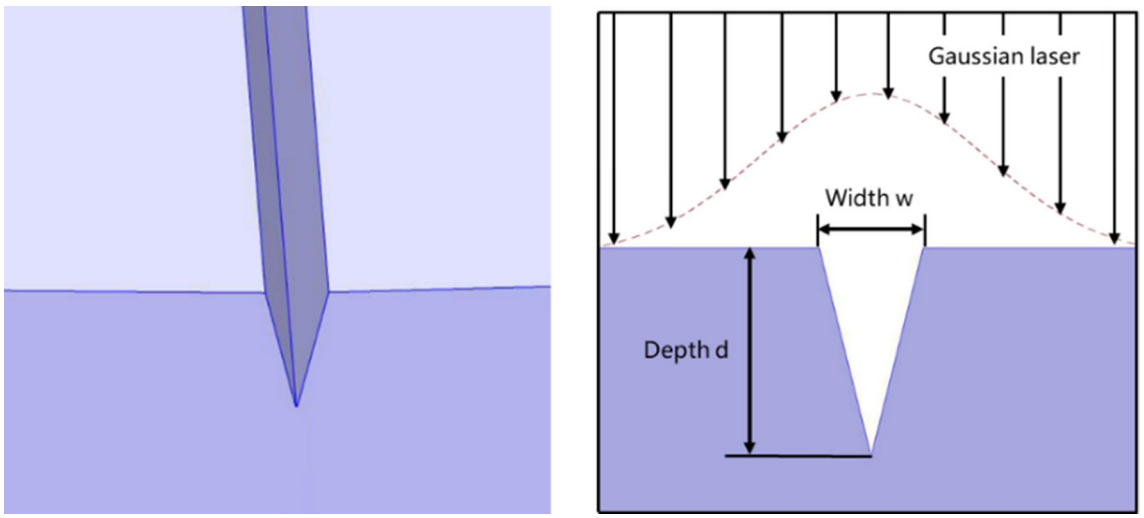

Fig. 2 V-groove microstructure for simulation

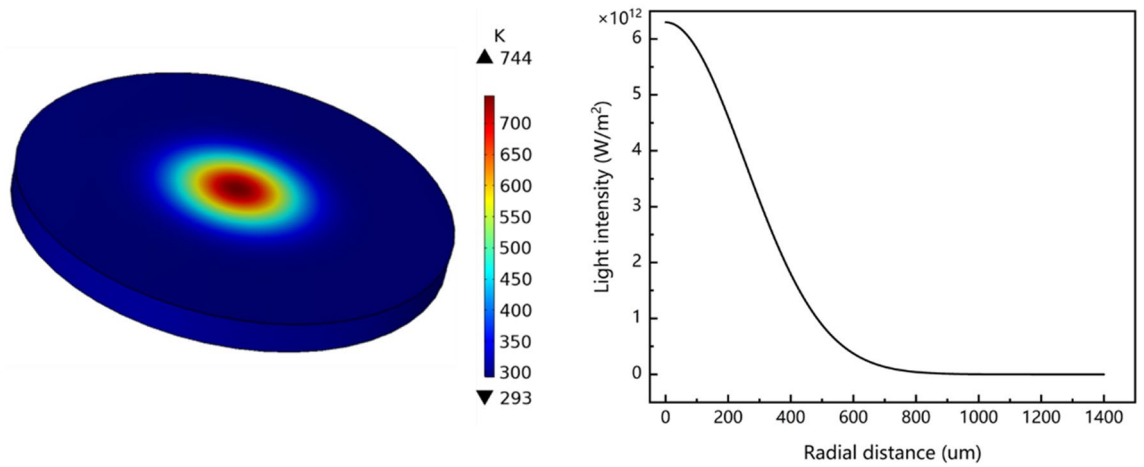

Fig. 3 Three-dimensional temperature distribution and radial light intensity distribution

distribution, consistent with Lambert's law that describes the law of laser propagation in the matter.

3 Results and discussion

Take the V- groove size as depth $d = 1$ μm, width $w = 0.5$ μm, and the energy density of the loaded laser as 6 J/cm^2 as an example for simulation. The temperature distribution inside the device at laser pulse width of 6 ns is presented in Fig. 4. Due to the presence of the V-shaped notch, the laser propagation direction changes. The laser propagating downward is refracted to both sides by the sidewalls of scratch, which superimposes and attenuates with the laser propagating vertically. Temperature streaks appear on both sides of the groove. The light and dark temperature bands showing similar diffraction patterns are distributed on the left and right sides of the V- groove. When multiple tracks are arranged, the sudden change in stress caused by the temperature difference will be alleviated because of the influence of each other.

Figures 5 and 6 illustrate isotherm distribution and electric field distribution after laser irradiation, respectively. It is evident that the bands formed by the isotherms almost coincide with the electric field stripes. This phenomenon illustrates the dependence of the temperature distribution inside a transparent dielectric material such as black glass on the internal electric field. When the V-groove modulates the light or electric field, the intensity of the electric field is enhanced in some areas, which will bring about an increase in temperature. Although the maximum temperature has not yet reached the melting point of 1750 K, the internal stresses caused by the thermal inhomogeneity are of concern.

On the one hand, the effect of width w on the thermal field is studied. The depth $d = 1$ μm is unchanged but width w variety. The scratch width w increased from 0.1 to 6 μm, with 0.1–1 μm at intervals of 0.1 μm and 1 μm to 6 μm at intervals of 1 μm. It can be seen from Fig. 7 that as the width w increases, the maximum temperature increases first and then decreases and reaches a peak when $w = 2$ μm. Because when w is tiny, the laser passes through the V-shaped groove and occurs the diffraction effect. As the width w increases, the diffraction effect gradually decreases, and the temperature increases. When w is more than 2 μm, the laser light is reflected the outside by the groove after being reflected twice. As w increases, more and more laser energy is reflected, and the material absorbs minor energy, and the maximum temperature decreases. The maximum temperature is far below the material's melting point of 1750 K, but its extreme points require attention.

On the other hand, the relationship between depth d and temperature is drawn in Fig. 8. The width remains the same at 0.5 μm. And the depth d is increased from 0.1 to 6 μm, with 0.1–1 μm at intervals of 0.1 μm and 1–6 μm at intervals of 1 μm. From Fig. 8, the temperature change curve shows that as the depth d increases, the maximum temperature increases first and then stabilizes. When the depth d is minor, the affected area is small, diffractive as the central part. As the depth d increases, the diffraction effect weakens, the slope increases, the place where laser modulation occurs, and the maximum temperature line show an increasing trend. However, at the same time, the slope increases, and heat transfer is more likely to occur. In the end, the modulation effect and heat conduction reach a balance. To sum up, the maximum temperature is far below the material's melting point of 1750 K.

As can be seen in Fig. 9, the maximum temperature in the model changes as the width and depth of the V-groove change. It is noteworthy that the temperature gradient is most pronounced at a depth-to-width ratio of 1/2. The

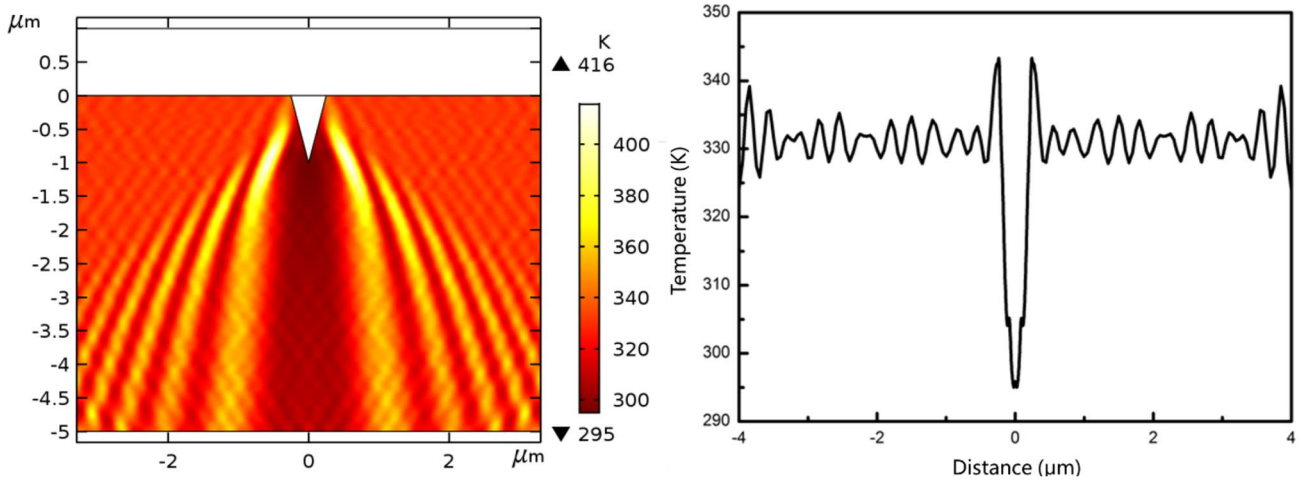

Fig. 4 Temperature profile and temperature curve at the scratch

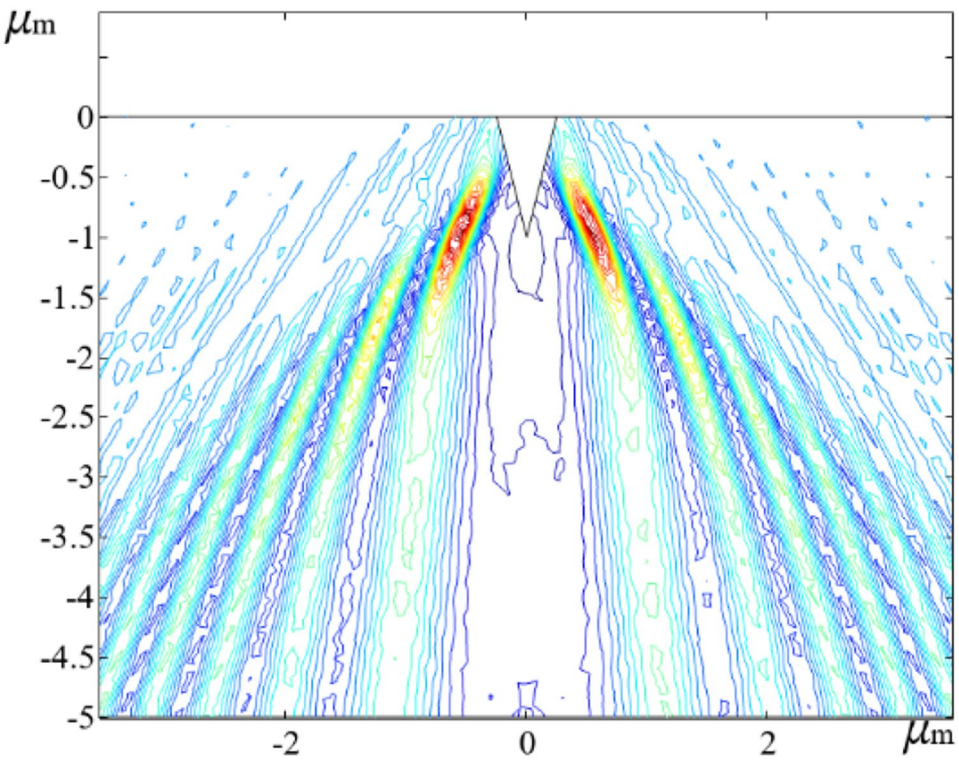

Fig. 5 The isothermal map of component

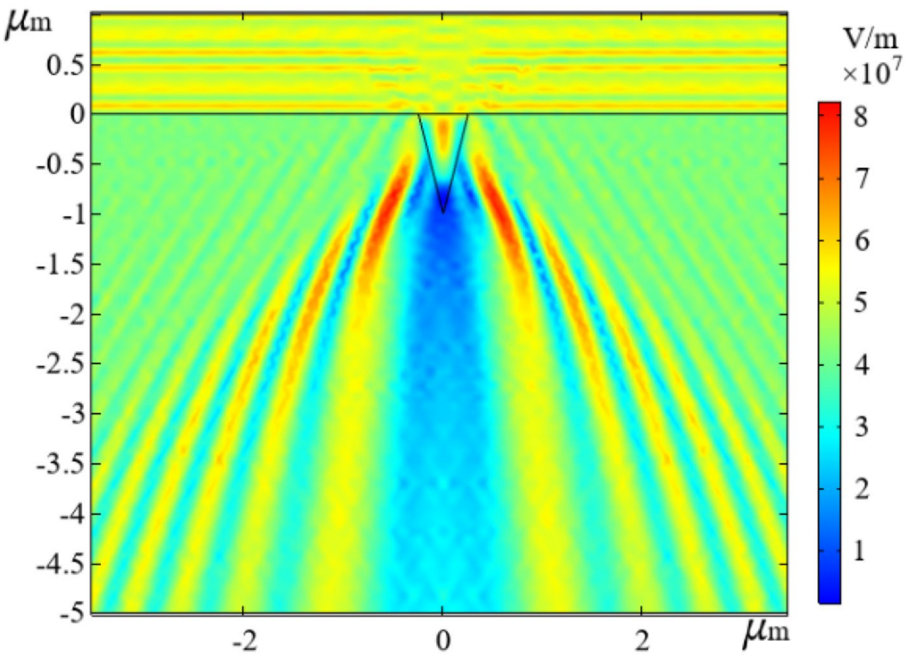

Fig. 6 The electric field of component

maximum temperature rises significantly with increasing V-groove size. In some scholarly studies of the relationship between slits and laser damage thresholds [16], slits with large aspect ratios significantly reduce the damage threshold of the optical element, which in turn is highly likely to cause an increase in the ablated area. From the information presented in Fig. 9, the main factor for damage to slits is not the high temperature but rather the stress concentration.

The complex mechanism of laser-matter interaction involves various physical processes occurring on a nanosecond timescale. The causes of laser ablation vary due to different materials and structures. The heat flux is usually

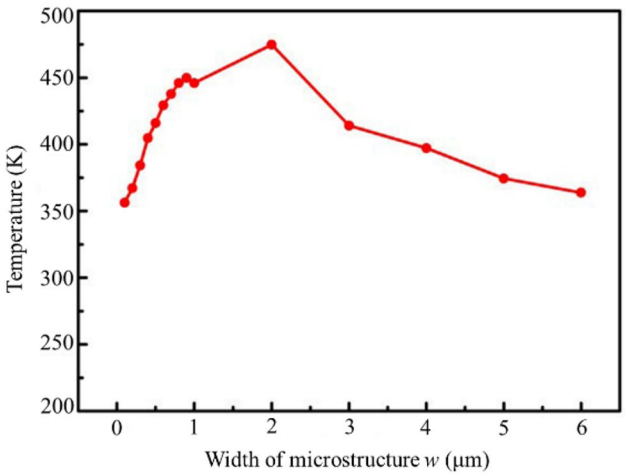

Fig. 7 Relationship between maximum temperature and groove width

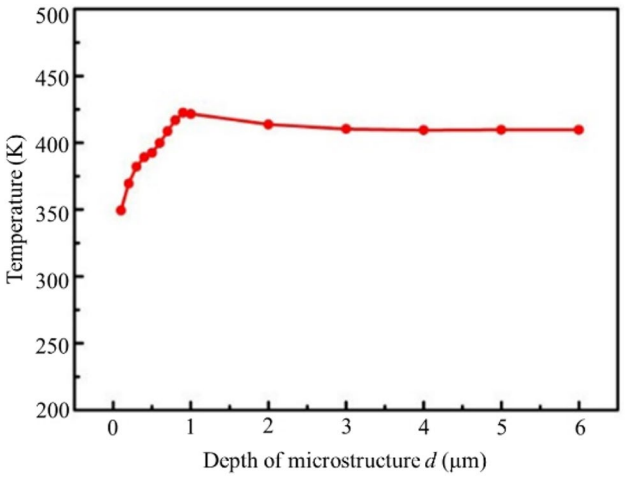

Fig. 8 Relationship between maximum temperature and groove depth

applied as a heat source and loaded directly onto the surface in laser irradiation models of materials like aluminum alloys and alumina [22]. However, when the microstructure plays a role, such as modulation of the laser, a single heat source to simulate heat transfer is no longer sufficient. In this paper, the converting electromagnetic losses into a heat source was considered, and the simulated thermal field has similar stripes to the electric and optical fields. This phenomenon could indicate that the thermal field in a dielectric material is more dependent on the distribution of the electric field instead of the heat source in previous studies. The mechanism of laser action under realistic conditions encompasses a complex set of effects that deserve further exploration and discovery.

4 Conclusion

The influence of the width and depth of microstructure on the thermal field was studied, respectively, and combined the two factors obtained the simulation results. The results show that microstructure has a significant influence on laser ablation of the absorption glass surface. It can be concluded as follows:

1. The model in this paper verifies the effect of microstructure on the thermal field of the absorbing glass under laser loading. The structure of the V- groove can easily cause the temperature concentration at the tip of the two sides. Still, the temperature at the bottom is lower than that of the crest. The resultant sharp temperature changes lead to high stresses.
2. The high-temperature points are mainly generated at the outer tips when the laser-irradiated on the surface with microstructure. These tips are vulnerable and need

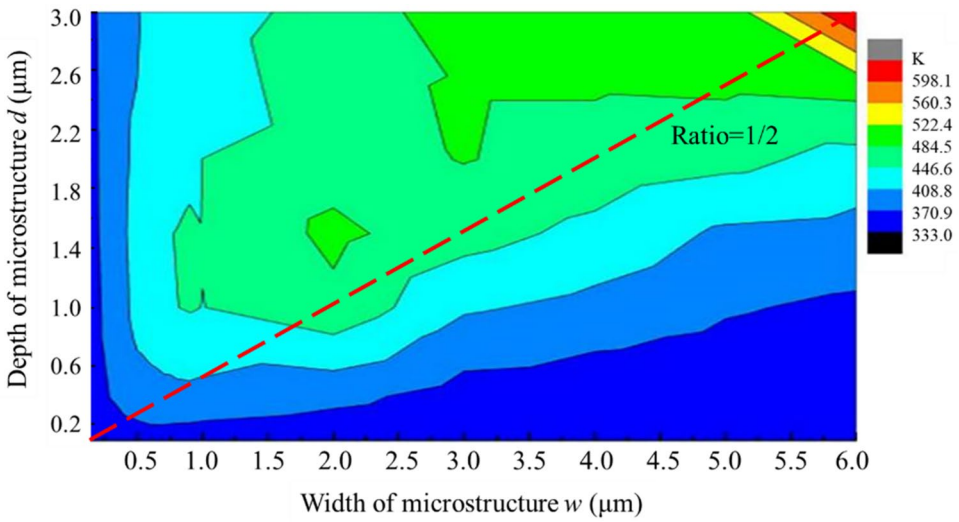

Fig. 9 The temperature distribution in the simulation various depth-width of the microstructure

protection from ablation and fracture in the design of microstructure arrays. This paper's model may give a good hint to solve the problem.

3. It can be drawn that both width and depth affect temperature, respectively. The impact of width is more noticeable than the impact of depth. When the two factors interact, there is a particular depth-width ratio zone where the temperature rises more quickly. The depth-width ratio is 0.5. This result will be utilized to create optimum structures when building a microstructures array.

Acknowledgements We would like to thank the National Natural Science Foundation of China (51535003, 51505331), the Natural Science Foundation of Heilongjiang Province in China (E2015007), the Harbin Outstanding Youth Science Fund (2015RAYGJ002), the Project for high-level talents of Bengbu University (BBXY2019KYQD01) and the Funds for the Central Universities (Grant No. HIT.NSRIF.2012036) for their financial supports.

References

1. L.M. Lidsky, Inertial confinement fusion—Review series. J. Fusion Energy **1**(3), 219–219 (1981)
2. R. Betti, O. Hurricane, Inertial-confinement fusion with lasers. Nature Phys. **12**, 435–448 (2016). https://doi.org/10.1038/nphys3736
3. E.I. Moses, Ignition on the national ignition facility. J. Phys. Conf. Series **112**(1), 012003 (2008)
4. J. Yin, Y. Cao, Research of laser-induced damage of aluminum alloy 5083 on micro-arc oxidation and composite coatings treatment. Opt. Express **27**(13), 18232 (2019)
5. P. Hed, D.F. Edwards, J.B. Davis, Subsurface damage in optical materials: origin, measurements and removal. in *Collected papers from ASPE Spring Conference on subsurface damage in glass* (1989)
6. T. Suratwala, M. Feit, W. Steele et al., Microscopic removal function and the relationship between slurry particle size distribution and workpiece roughness during pad polishing. J. Am. Ceram. Soc. **97**(1), 81–91 (2014)
7. K. Wilhelmsen, A. Awwal, G. Brunton et al., 2011 Status of the automatic alignment system for the national ignition facility. Fusion Eng. Des. **87**(12), 1989–1993 (2012)
8. E.I. Moses, The National Ignition Facility and laser fusion energy. in *2011 International Quantum Electronics Conference (IQEC) and Conference on Lasers and Electro-Optics (CLEO) Pacific rim Incorporating the Australasian Conference on Optics, Lasers and Spectroscopy and the Australian confErence on Optical Fibre Technology*. IEEE, 2012.
9. R.A. Hawleyfedder, C.J. Stolz, J.A. Menapace et al., *NIF optical materials and fabrication technologies: an overview*.in Proceedings of SPIE - The International Society for Optical Engineering, 2004, vol. 5341, pp. 102–5.
10. A. Pereira, J.G. Coutard, S, Becker, et al., Impact of organic contamination on 1064-nm laser-induced damage threshold of dielectric mirrors.in *Laser-Induced Damage in Optical Materials: 2006. International Society for Optics and Photonics*, 2007, vol. 6403, p.64030I.
11. C.R. Giuliano, Laser-induced damage to transparent dielectric materials. Appl. Phys. Lett. **5**(7), 137–139 (1964)
12. N. Bloembergen, Role of cracks, pores, and absorbing inclusions on laser-induced damage threshold at surfaces of transparent dielectrics. Appl. Opt. **12**(4), 661–664 (1973)
13. B. Lawn, R. Wilshaw, Indentation fracture: principles and applications. J. Mater. Sci. **10**(6), 1049–1081 (1975)
14. F.Y. Genin, A. Salleo, T.V. Pistor et al., role of light intensification by cracks in optical breakdown on surfaces. J Opt Soc Am A Opt Image Sci Vis **18**(10), 2607–2616 (2001)
15. A.M. Rubenchik, M.D. Feit, Initiation, growth, and mitigation of UV-laser-induced damage in fused silica.in *Laser-Induced Damage in Optical Materials: 2001. International Society for Optics and Photonics*, 2002, vol. 4679, pp. 79–95.
16. M.D. Feit, A.M. Rubenchik. Influence of subsurface cracks on laser-induced surface damage.*in Laser-induced damage in optical materials: 2003. International Society for Optics and Photonics*, 2004, vol. 5273, pp. 264–272.
17. P. Fan, M. Zhong, L. Li et al., Rapid fabrication of surface micro/nano structures with enhanced broadband absorption on Cu by picosecond laser. Opt. Express **21**(10), 11628–11637 (2013)
18. M. Huang, F. Zhao, Y. Cheng et al., The morphological and optical characteristics of femtosecond laser-induced large-area micro/nanostructures on GaAs, Si, and brass. Opt. Express **18**(104), A600–A619 (2010)
19. A.Y. Vorobyev, C. Guo, Femtosecond laser blackening of platinum. J. Appl. Phys. **104**(5), 053516 (2008)
20. A.Y. Vorobyev, C. Guo, Colorizing metals with femtosecond laser pulses. Appl. Phys. Lett. **92**(4), 041914 (2008)
21. A.Y. Vorobyev, A.N. Topkov, O.V. Gurin et al., Enhanced absorption of metals over ultrabroad electromagnetic spectrum. Appl. Phys. Lett. **95**(12), 121106 (2009)
22. J. Yin, Y. Cao, Y. Yan et al., Laser-induced damage of black glass before and after surface treatment by containing impurities-SiO2 film during ultra clean manufacturing. J. Clean. Prod. **257**, 120360 (2020)